Prabha Materials Science Letters
Vol. 4, No. 2, 170-178, 2025
https://doi.org/10.33889/PMSL.2025.4.2.016

Ram Arti Publishers

Luminescence of Eu^{3+}/Eu^{2+} In PVA Film: Transitions from the $^5D_0$ Level and its Lifetime Measurement

Muskan Sahu
Physics Department,
Bundelkhand University, Jhansi, 284001, Uttar Pradesh, India.
Corresponding author: muskansahuangel@gmail.com

R. K. Verma
Physics Department,
Bundelkhand University, Jhansi, 284001, Uttar Pradesh, India.
E-mail: 2rajeshvermabhu12345@gmail.com

(Received on September 30, 2024; Revised on February 4, 2025; Accepted on February 20, 2025)

Abstract
We have synthesized Eu^{3+} doped poly vinyl alcohol (PVA) polymer film by the solution-casting method. The vibration features of the film are analyzed by using the FTIR spectrum. In the FTIR spectrum, many peaks are observed and correlate with different branches of vibrations. On excitation of 325 nm, Eu^{3+} ions emit at 579 nm, 592 nm, 615 nm, 649 nm, 698 nm through transitions $^5D_0 \rightarrow {}^7F_0$, $^5D_0 \rightarrow {}^7F_1$, $^5D_0 \rightarrow {}^7F_2$, $^5D_0 \rightarrow {}^7F_3$, $^5D_0 \rightarrow {}^7F_4$ respectively. These peaks are verified with the help of Eu^{3+} energy level diagram. In addition, we observed a broad peak of Eu^{2+} in the range 450 nm to 550 nm centered at 500 nm. Some stark splitting also has been observed in transitions $^5D_0 \rightarrow {}^7F_0$ and $^5D_0 \rightarrow {}^7F_4$. The micron - second lifetime of the $^5D_0$ level of Eu^{3+} is observed and correlated with the emission spectrum.

Keywords- Luminescence, Lifetime, PVA film.

1. Introduction

Nowadays, the world's energy deficiency has become increasingly prevalent day by day, and improving energy efficiency is a challenge to all scientific communities around the world. With the rapid growth of contemporary society, sustainable development of energy by the discovery of different types of materials may be full fill. We know human daily work and life, the demand for lighting power is a huge percentage of the total power consumption. But the already-invented good quality of the light emitting diode (LED), fluorescent and incandescent lamps have many shortcomings, for instance, high power consumption, short service lifespan, low energy conversion efficiency, and environmental pollution, which are inconsistent with the purpose of power economy and environmental protection under the present circumstances. In the present time, rare earth (RE)-doped materials have a lot of advantages and applications in different areas (Shahi et al., 2015; Wang et al., 2019; Moudam and Lakbita, 2021). Photonics, optoelectronics, laser materials, display panels, and light-emitting diodes are some of the best-suited areas and highly demanding for these materials (Peng et al., 2010; Dwivedi, 2023). The rare earth elements show excellent properties like very sharp bands, large Stokes shift, and long meta-stable states (Kumar et al., 2014; Bousrez et al., 2021). Sharp bands and large Stokes shift in rare earth materials are observed due to the 4f-4f forbidden transitions (Ram et al., 1984; Raju et al., 2006a; Kindrat and Padlyak, 2018).

Polymer matrixes are very fascinating luminescent materials due to their transparency and anisotropy Polyvinyl alcohol (PVA) is synthetic and hydrophilic in nature. It is also a biodegradable and low-hazardous polymer to the environment and the -OH group present in the polymer makes it suitable for interaction with different inorganic and organic-type materials (Alsaad et al., 2020; Saber et al., 2023). Its hydrophilic nature

Ram Arti Publishers

makes it a potential candidate for biomedical applications. PVA can also be used in coating and binding (Afshari et al., 2021). These materials are also useful in the optical fibre industry. PVA is semi-crystalline in nature, which is better than considering amorphous organic and inorganic materials (Peppas and Merrill, 1977). The refractive index (1.5) and tensile strength make it different from other materials (Matsumoto and Ohyanagi, 1958; Ghoshal et al., 2012).

Eu^{3+} is used as an activator for achieving red emission (Raju et al., 2006b; Ilmi et al., 2019). These emissions cover almost all red regions. The emission peaks observed in the case of Eu^{3+} through the transition between $^5D_0$ and ^7F_j (j = 0, 1, 2, 3, 4….) levels. The intense peak observed corresponds to the transition $^5D_0 \rightarrow {}^7F_2$, and another peak that is slightly less intense than the $^5D_0 \rightarrow {}^7F_2$ transition also appears. Transitions $^5D_0 \rightarrow {}^7F_2$ and $^5D_0 \rightarrow {}^7F_1$ are electric dipole and magnetic dipole transitions, respectively. The $^5D_0 \rightarrow {}^7F_3$ transition is forbidden according to the transition rule. $^5D_0 \rightarrow {}^7F_4$ transition is allowed transition and is dependent on the environment of the host materials. According to the electric dipole transition rule $\Delta J \leq 6$ and $\Delta S=0$, $\Delta L=\pm 1$. Transition from J=0 to J=0 is forbidden. For magnetic dipole transition: $\Delta S=0$, $\Delta J \leq 1$, $\Delta L=0$. Similarly for the magnetic dipole transition J=0 to J=0 transition is not allowed (Raju et al., 2006b; Kindrat and Padlyak, 2018).

In this paper, we have synthesized a Eu^{3+}-doped PVA film by the solution casting method. The vibrational features of the film are discussed with the help of FTIR. Eu^{3+} emission and rarely reported Eu^{2+} emissions are observed without any reducing atmosphere and high-temperature treatment of material, and the very small Stark splitting has been observed in transition $^5D_0 \rightarrow {}^7F_0$ and $^5D_0 \rightarrow {}^7F_4$. The lifetime of the $^5D_0$ level is measured and correlated with emission spectra.

2. Experimental Section

Pure Europium Nitrate [$Eu(NO_3)_3.6H_2O$] (M.W. 446.06), polyvinyl alcohol (M.W. 85000-124000), ethyl alcohol C_2H_5OH (99% pure), NaOH (M.W. 40), and Milli-Q water are used in the synthesis of material. The first solution, 0.01 mol% of $Eu(NO_3)_3$ and 10 ml of water, is prepared. The second solution of 0.9 g of PVA and 20 ml of water is prepared. Now mix both solutions in another beaker. We have used 1 N NaOH solution for pH balancing. The pH of the solution is maintained at 7. Stir continuously this mixture for 8 h at 40 °C; after 8 h of stirring, the polymer dissolves completely. The film of this solution is fabricated easily by the solution casting method (Raju et al., 2006b). The solution was poured into a petri dish for the fabrication of film. The film is prepared by slow evaporation, which helps in removing air bubbles that arise on the surface of the film. The synthesis diagram for the fabrication of Eu^{3+}: PVA film is shown in **Figure 1**.

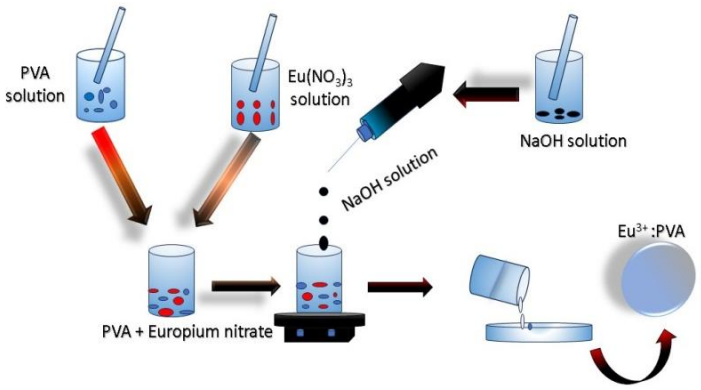

Figure 1. Synthesis process to obtain Eu^{3+} doped PVA film.

Fourier transform infrared (FTIR) RX-1 Spectrometer Perkin Elmer has been used for exploring the vibrational features of the Eu^{3+}/Eu^{2+}: PVA film. The emission spectra of the film have been obtained with the help of Photoluminescence spectrometer, LabRAM HR Evol, the film was excited with 325 nm laser.

3. Results and Discussion

3.1 FTIR Analysis

FTIR spectra of $Eu^{3+}/Eu^{2+:}$ PVA has been recorded in the range 4000 cm^{-1} to 400 cm^{-1} at room temperature. The film was mounted directly on a sample holder for the measurements. In the range 3200–3000 cm^{-1}, a broadband has been observed. This broad band is centred around 3368.57 cm^{-1} and corresponds to O-H symmetric vibrations (Singh et al., 2013). PVA consists of an OH group; this band is due to the hydrogen bond-forming capability of PVA (Blout and Karplus, 1948; Mansur et al., 2008). Also signifies the hydrophilic nature of PVA. One peak is observed at 2655.24 cm^{-1}, and this is due to the weak antisymmetric stretching vibration of C-H mode. The C=C band has been observed at 1637.98 cm^{-1} due to the acetyl group. CH_2 bending and CH_2 wagging vibrations are observed at 1508.11 cm^{-1} and 1353.60 cm^{-1}. The peak at around 1227.39 cm^{-1} is due to stretching vibrations of the C=O mode of the alcohol group. C-C vibrations observed at 1032 cm^{-1}. CH_2 stretching vibration observed at 897.48 cm^{-1}. The FTIR spectra of Eu^{3+}-doped film are shown in **Figure 2**.

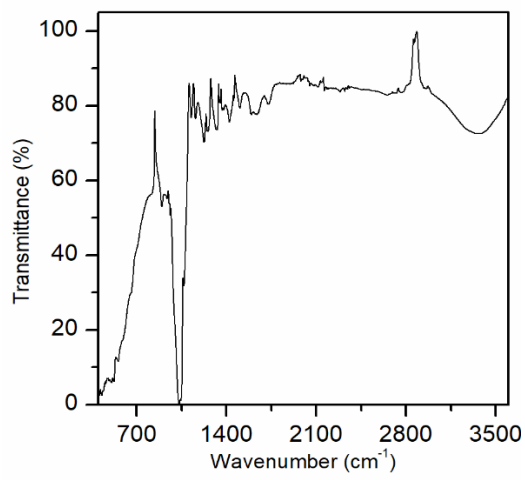

Figure 2. FTIR spectra of Eu^{3+} doped PVA film.

3.2 Photoluminescence Spectra Analysis

According to reported literature, the excitation spectra of Eu^{2+} shows broad peaks around 320 nm and 370 nm and Eu^{3+} show sharp peaks ranges from 350 nm to 550 nm (Liu et al., 2023). We have recorded the emission of Eu^{3+}/Eu^{2+}: PVA film on excitation of 325 nm laser source. Five peaks are observed in the photoluminescence spectra. These transitions are actually due to the 4f-4f transition. The peak positions are observed at 579 nm, 592 nm, 615 nm, 649 nm and 698 nm corresponding to the transition $^5D_0 \rightarrow {}^7F_0$, $^5D_0 \rightarrow {}^7F_1$, $^5D_0 \rightarrow {}^7F_2$, $^5D_0 \rightarrow {}^7F_3$ and $^5D_0 \rightarrow {}^7F_4$, respectively. The transitions, $^5D_0 \rightarrow {}^7F_{5,6,7}$ do not show significant intensity which lies in infrared regions. The transition $^5D_0 \rightarrow {}^7F_0$ is more important and gives information related to localized symmetry around the Eu^{3+} ion (Mani et al., 2018). The transitions $^5D_0 \rightarrow {}^7F_{2,4,6}$ are allowed by the electric dipole transitions rule because here $\Delta J \leq 6$. The transition $^5D_0 \rightarrow {}^7F_1$ is allowed by magnetic dipole transition and corresponds to the transition rule $\Delta J = 1$, $\Delta L = +1$. The emission intensity corresponds to the transition $^5D_0 \rightarrow {}^7F_2$ is maximum and it is hypersensitive electric dipole transition and very much influenced by the polymer host. The change in the host matrix will result in more or less intense

electric dipole transition due to the change in the center of symmetry around Eu^{3+}. An intense peak at 442 nm is observed due to the transition $^5D_4 \rightarrow {}^7F_6$. Some less intense peaks have been observed due to the transitions from $^5D_2$ level. These transitions don't have very high transitional intensity due to this these transitions are not of great interest. The emission spectrum is shown in **Figure 3**.

The partial energy level diagram of Eu^{3+} is shown in **Figure 4**. When Eu^{3+}/Eu^{2+} doped PVA film is excited by 325 nm laser source, electrons are then promoted from $^7F_0$ to $^5H_3$ level. The electron further makes multiple non-radiative transitions and then populate to metastable state $^5D_0$. Then again, it makes several radiative transitions from $^5D_0$ level to ^7F_J (J = 0, 1, 2, 3, etc.) levels, and is shown in **Figure 4**.

Additionally, we have observed a broad peak in the UV region in the wavelength range 450 nm to 550 nm, and this broadband is centered at 500 nm as shown in **Figure 5**. The peak is rarely reported in literature. This broadband is less intensive compared to the $^5D_0 \rightarrow {}^7F_2$ transition. This band appeared in PL spectra due to transition $4f^6 5d^1 \rightarrow 4f^7(^8S_{7/2})$ which is allowed by electrostatic dipole transition, and another paper also reports the peak of the Eu^{2+} ion in different host matrixes (Yanmin et al., 2009; Yu et al., 2013; Grandhe et al., 2011). The occurrence of this band in the PL spectra of Eu^{3+}: PVA shows the reduction of a small amount of Eu^{3+} ions into Eu^{2+} ions without any reducing atmosphere. In most of the research papers that have been published some reducing agents like N_2/H_2 and CO have been used for changing the valency of the europium ion from the trivalent state to the divalent state. This type of reduction can also be achieved at high temperatures in the presence of air according to reported literature (Grandhe et al., 2011). There is already reported-literature related to the reduction of Eu^{3+} to divalent europium ion at room temperature without any reducing atmosphere (Morales–Saavedra et al., 2022). In the present research work, we have observed reduction of Eu^{3+}into Eu^{2+} at room temperature without using any reducing agent. Intensity of broad peak is less compared to sharp peaks indicating, reduction in form of Eu^{2+} is not efficient. The reason for the reduction of Eu^{3+} is the interaction between the cations Eu^{3+} and oxygen present in the hydroxyl group of PVA, this oxygen transfer electron to the Eu^{3+} and converted into Eu^{2+} (Hernández-Fuentes et al., 2025).

From the PL spectra, it can be observed that there is some stark splitting in the $^5D_0 \rightarrow {}^7F_0$ transition and $^5D_0 \rightarrow {}^7F_4$ transition. The presence of these peaks also supports the presence of the field in PVA film.

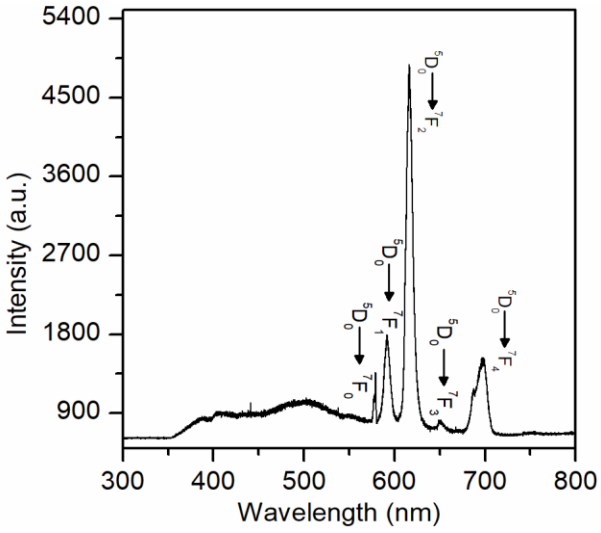

Figure 3. Photoluminescence spectra of Eu^{3+}: PVA film under the excitation source of 325 nm.

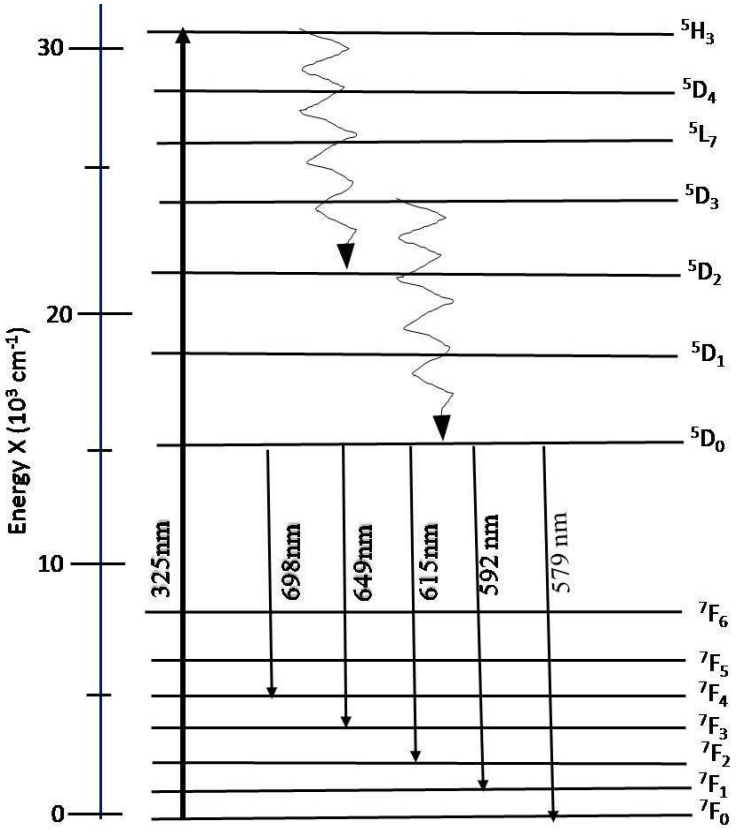

Figure 4. Partial energy level diagram of Eu^{3+} ions.

The full width at half maxima (FWHM) of the peaks have been shown in **Table 1**. The FWHM of the $^5D_0 \rightarrow {}^7F_2$ transition is very low and about 9 nm. The FWHM of the $^5D_0 \rightarrow {}^7F_4$ transition is maximum, and it is about 25 nm. The transitions $^5D_0 \rightarrow {}^7F_0$ and $^5D_0 \rightarrow {}^7F_3$ do not show significant FWHM.

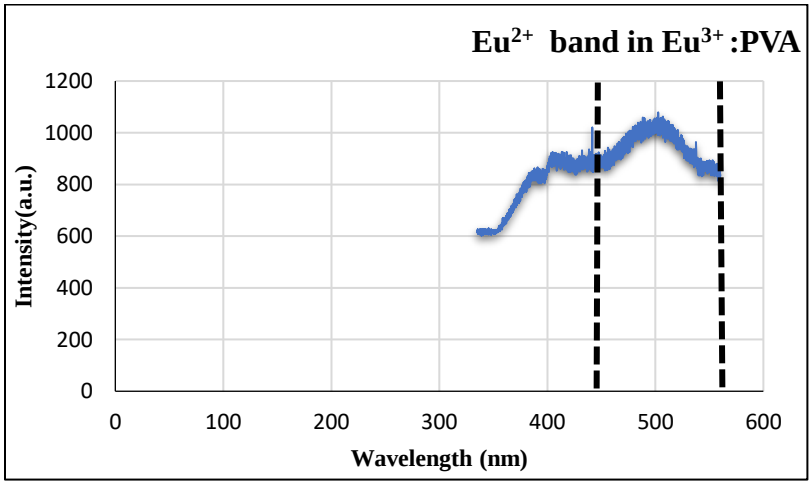

Figure 5. Eu^{2+} emission in PVA film.

Table 1. The full width at half maximum corresponds to λ_{max} peak emission in photoluminescence in Eu^{3+}/Eu^{2+}: PVA.

Transitions	λ_{max} (nm)	FWHM (nm)
$^5D_0 \rightarrow {}^7F_0$	579 nm	Less intense
$^5D_0 \rightarrow {}^7F_1$	592 nm	15 nm
$^5D_0 \rightarrow {}^7F_2$	615 nm	9 nm
$^5D_0 \rightarrow {}^7F_3$	649 nm	Less intense
$^5D_0 \rightarrow {}^7F_4$	698 nm	25 nm

The transition $^5D_0 \rightarrow {}^7F_2$ is very sharp. The sharpness of each peak creates a space to measure the monochromaticity. The monochromaticity of transition can be determined by the R-value. R-value is the ratio of the intensity of hypersensitive transitions $^5D_0 \rightarrow {}^7F_2$ and $^5D_0 \rightarrow {}^7F_1$ transition. R-value also helps in measuring the lanthanide site symmetry (Mani et al., 2018).

$$\text{R Value} = I(^5D_0 \rightarrow {}^7F_2)/I(^5D_0 \rightarrow {}^7F_1) = 2.5.$$

The R -value is not very high this indicates a higher symmetry in the vicinity of Eu^{3+} in the PVA film. The sharpness of the transitions make it different from simple Eu^{3+} transitions in different host materials and may be useful for laser materials.

3.3 Color Chromaticity

The commission international d'Eclairge (CIE) 1931 diagram with (x, y) co-ordinates is shown in **Figure 6**. The chromaticity co-ordinate of Eu^{3+}/Eu^{2+} :PVA film is (0.381, 0.331) which appear some what white and red region. For only Eu^{3+} chromaticity co-ordinates (x, y) must be in the red region but due to the contribution of broad band of Eu^{2+} ion in the region 450 nm- 550 nm this shifting has been occurred in the PVA film (Secu and Secu, 2020; Nandimath et al., 2021).

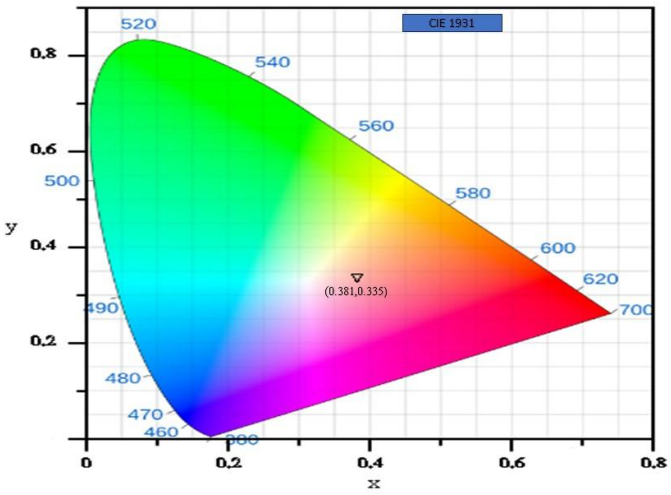

Figure 6. CIE monochromaticity diagram of Eu^{3+}/Eu^{2+}:PVA film.

3.3 Life Time Decay Measurement

The decay curve of Eu^{3+}/Eu^{2+}: PVA film is investigated by monitoring the emission of 615 nm under the excitation of 325 nm. The curve is shown in **Figure 7**. The curve is best fitted by the exponential decay type function. The lifetime is calculated with the relation between intensity and time.

$$I = A \exp(\frac{-t}{\tau}).$$

Here, I is the luminescence intensity, A is constant, t is the time and $\boldsymbol{\tau}$ is the lifetime for the exponential component.

Luminescence decay time $\boldsymbol{\tau}$ depends on radiative lifetime $\boldsymbol{\tau}_{rad}$ and multi -phonon relaxation rate A_p.

$$\boldsymbol{\tau}^{-1} = \boldsymbol{\tau}^{-1}_{rad} + A_p.$$

The lifetime that has been observed here is 110 μs. The micron second life time may be useful in different areas like display devices, biosensing, laser material, etc.

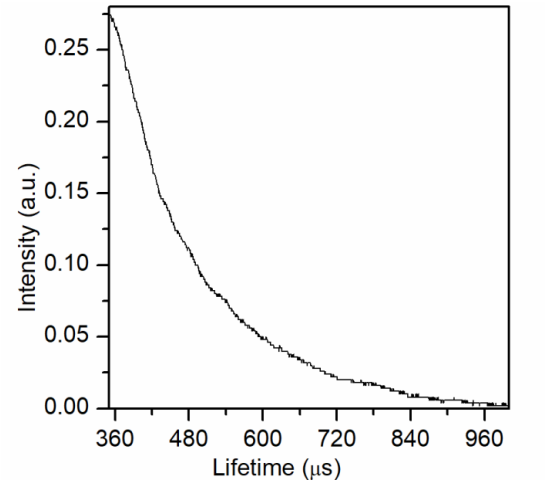

Figure 7. Lifetime of Eu^{3+}: PVA film.

4. Conclusions

To summarise, we synthesized Eu^{3+}/Eu^{2+}: PVA film and investigated the luminescence, mono-chromaticity and can be correlated with the local environment of Eu^{3+} ions. Different branches of vibration are analyzed by the FTIR spectrum. We observe O-H, C-H, and C-C modes of vibration in the PVA film. By irradiating with light at 325 nm, the sample showed a strong red emission at 579 nm, 592 nm, 615 nm, 649 nm, 698 nm through transitions $^5D_0 \rightarrow {}^7F_0$, $^5D_0 \rightarrow {}^7F_1$, $^5D_0 \rightarrow {}^7F_2$, $^5D_0 \rightarrow {}^7F_3$, $^5D_0 \rightarrow {}^7F_4$ respectively, mainly resulting from the $^5D_0 \rightarrow {}^7F_2$ transition. Additionally, we observed a broad peak in the range 450 nm to 550 nm due to Eu^{2+} emission. Lifetime also recorded 110μs which is good for optical panel display applications and sensing purposes.

Conflict of Interest

There are no conflicts of interest to declare.

AI Disclosure

The author(s) declare that no assistance is taken from generative AI to write this article.

Acknowledgments

Authors are thankful to the innovation center, Bundelkhand University, Jhansi, for FTIR spectra. Authors are also thankful to UGC for startup grant No. F.30-11/2014(BSR) and Bundelkhand University for seed money.

References

Afshari, M., Mohammadloo, H.E., Sarabi, A.A., & Roshan, S. (2021). Modification of hydroxyapatite-based coating in the presence of polyvinylalcohol (PVA) for implant application: corrosion, structure and surface study. *Corrosion Science*, *192*, 109859.

Alsaad, A.M., Ahmad, A.A., Al Dairy, A.R., Al-anbar, A.S., & Al-Bataineh, Q.M. (2020). Spectroscopic characterization of optical and thermal properties of (PMMA-PVA) hybrid thin films doped with SiO_2 nanoparticles. *Results in Physics*, *19*, 103463.

Blout, E.R., & Karplus, R. (1948). The infrared spectrum of polyvinyl alcohol. *Journal of the American Chemical Society*, *70*(2), 862-864.

Bousrez, G., Renier, O., Paterlini, V., Smetana, V., & Mudring, A.V. (2021). Magnetic, photo-and electroluminescent: multifunctional ionic tb complexes. *Inorganic Chemistry*, *60*(23), 17487-17497.

Dwivedi, Y. (2023). Comparative spectroscopic study of Tb: Ce $(Sal)_3$Phen complex inhibited PVA nanofibres for flexible moisture sensor. *Spectrochimica Acta Part A: Molecular and Biomolecular Spectroscopy*, *302*, 123078.

Ghoshal, S., Denner, P., Stapf, S., & Mattea, C. (2012). Study of the formation of poly (vinyl alcohol) films. *Macromolecules*, *45*(4), 1913-1923.

Grandhe, B.K., Bandi, V.R., Jang, K., Kim, S.S., Shin, D.S., Lee, Y.I., Lim, J.M., & Song, T. (2011). Reduction of $Eu^{3+}$to Eu^{2+} in $NaCaPO_4$: Eu phosphors prepared in a non-reducing atmosphere. *Journal of Alloys and Compounds*, *509*(30), 7937-7942.

Hernández-Fuentes, C.F., Carrera-Jota, M.L., Hernández, M.G., Juárez-López, F., Roque-de la Puente, J., & de Jesús, Á.M.R. (2025). Luminescent study of Eu (OOCC6H5) 3·3 (H2O) complex dispersed on polyvinyl alcohol films: crystal structure, interaction and quenching effect. *Journal of Molecular Structure*, *1322*, 140296.

Ilmi, R., Anjum, S., Haque, A., & Khan, M.S. (2019). A new brilliant red emitting Eu (III) ternary complex and its transparent flexible and photostable poly (urethane) hybrid thin film for optoelectronic applications. *Journal of Photochemistry and Photobiology A: Chemistry*, *383*, 111968.

Kindrat, I.I., & Padlyak, B.V. (2018). Luminescence properties and quantum efficiency of the Eu-doped borate glasses. *Optical Materials*, *77*, 93-103.

Kumar, K.N., Sivaiah, K., & Buddhudu, S. (2014). Structural, thermal and optical properties of Tb^{3+}, Eu^{3+} and co-doped (Tb^{3+}+ Eu^{3+}): PEO+ PVP polymer films. *Journal of Luminescence*, *147*, 316-323.

Liu, L., Shao, X., Zhang, Z., Liu, J., Hu, Y., & Zhu, C. (2023). Spectral properties and self-reduction of Eu $^{3+}$ to Eu $^{2+}$ in aluminosilicate oxyfluoride glass. *RSC Advances*, *13*(34), 23708-23715.

Mani, R., Jiang, H., Gupta, S.K., Li, Z., & Duan, X. (2018). Role of synthesis method on luminescence properties of europium (II, III) ions in β-Ca_2SiO_4: probing local site and structure. *Inorganic Chemistry*, *57*(3), 935-950.

Mansur, H.S., Sadahira, C.M., Souza, A.N., & Mansur, A.A. (2008). FTIR spectroscopy characterization of poly (vinyl alcohol) hydrogel with different hydrolysis degree and chemically crosslinked with glutaraldehyde. *Materials Science and Engineering: C*, *28*(4), 539-548.

Matsumoto, M., & Ohyanagi, Y. (1958). Refractive index of dilute aqueous solution of polyvinyl alcohol. *Journal of Polymer Science*, *31*(122), 225-227.

Morales–Saavedra, O.G., Chavira, E., Rodríguez-Rosales, A.A., Flores-Flores, J.O., Mata-Zamora, M.E., & Ponce, P. (2022). Sharp luminescent violet-and blue-emitting stable (Eu^{3+}→ Eu^{2+}: PPA): SiO_2sonogel hybrid glasses: Synthesis, structural and overall photophysical characterizations. *Optical Materials*, *123*, 111760.

Moudam, O., & Lakbita, O. (2021). Potential end-use of a europium binary photoluminescent ink for anti-counterfeiting security documents. *ACS Omega*, *6*(44), 29659-29663.

Nandimath, M., Bhajantri, R.F., & Naik, J. (2021). Spectroscopic and color chromaticity analysis of rhodamine 6G dye-doped PVA polymer composites for color tuning applications. *Polymer Bulletin*, *78*, 4569-4592.

Peng, H., Stich, M.I., Yu, J., Sun, L.N., Fischer, L.H., & Wolfbeis, O.S. (2010). Luminescent europium (III) nanoparticles for sensing and imaging of temperature in the physiological range. *Advanced Materials*, *22*(6), 716-719.

Peppas, N.A., & Merrill, E.W. (1977). Development of semicrystalline poly (vinyl alcohol) hydrogels for biomedical applications. *Journal of Biomedical Materials Research*, *11*(3), 423-434.

Raju, G.S.R., Buddhudu, S., & Rajulu, A.V. (2006b). Red emission from Eu^{3+}: PVA polymer film. *Journal of Applied Polymer Science*, *102*(4), 3273-3276.

Raju, G.S.R., Buddhudu, S., Rajulu, A.V., & Devi, L.G. (2006a). Emission spectra of Tb^{3+}: PVA polymer films. *Spectroscopy Letters*, *39*(5), 487-495.

Ram, S., Lamba, O.P., & Bist, H.D. (1984). Optical transitions of Eu^{3+} ions in $EuCl_3$ solutions. *Pramana*, *23*, 59-68.

Saber, S., El-Sayed, S., & El Sayed, A.M. (2023). Influence of Eu^{3+} on the structural, optical and electrical properties of PEO–PVA: Dual bandgap materials for optoelectronic applications. *Journal of Materials Science: Materials in Electronics*, *34*(5), 406. https://doi.org/10.1007/s10854-023-09841-6.

Secu, M., & Secu, C.E. (2020). Processing and optical properties of Eu-doped chloroborate glass-ceramic. *Crystals*, *10*(12), 1101. https://doi.org/10.3390/cryst10121101.

Shahi, P.K., Singh, A.K., Rai, S.B., & Ullrich, B. (2015). Lanthanide complexes for temperature sensing, UV light detection, and laser applications. *Sensors and Actuators A: Physical*, *222*, 255-261.

Singh, J.P., Dixit, G., Srivastava, R.C., Negi, P., Agrawal, H.M., & Kumar, R. (2013). HRTEM and FTIR investigation of nanosized zinc ferrite irradiated with 100 MeV oxygen ions. *Spectrochimica Acta Part A: Molecular and Biomolecular Spectroscopy*, *107*, 326-333.

Wang, H., Fang, L., Zhang, Z., Epaarachchi, J., Li, L., Hu, X., Lu, C., & Xu, Z. (2019). Light-induced rare earth organic complex/shape-memory polymer composites with high strength and luminescence based on hydrogen bonding. *Composites Part A: Applied Science and Manufacturing*, *125*, 105525.

Yanmin, Q., Zhang, X., Xiao, Y.E., Yan, C., & Hai, G. (2009). Photoluminescent properties of Sr_2SiO_4: Eu^{3+} and Sr_2SiO_4: Eu^{2+} phosphors prepared by solid-state reaction method. *Journal of Rare Earths*, *27*(2), 323-326.

Yu, H., Deng, D., Zhou, D., Yuan, W., Zhao, Q., Hua, Y., Zhao, S., Huang, L., & Xu, S. (2013). $Ba_2Ca(PO_4)_2$: Eu^{2+} emission-tunable phosphor for solid-state lighting: luminescent properties and application as white light emitting diodes. *Journal of Materials Chemistry C*, *1*(35), 5577-5582.